

Removal of Congo red and Mordant Dyes via Photodegradation Using ZnO/Fe₂O₃ Nanocomposite

Sponza DT*

Department Environmental Sciences, Faculty of Engineering Environmental Engineering, Turkey

*Corresponding author:

Delia Teresa Sponza,
Department Environmental Sciences, Faculty of
Engineering Environmental Engineering, Turkey

Received: 28 July 2023

Accepted: 04 Sep 2023

Published: 11 Sep 2023

J Short Name: AJSCCR

Copyright:

©2023 Sponza DT, This is an open access article distributed under the terms of the Creative Commons Attribution License, which permits unrestricted use, distribution, and build upon your work non-commercially.

Citation:

Sponza DT. Removal of Congo red and Mordant Dyes via Photodegradation Using ZnO/Fe₂O₃ Nanocomposite. *Ame J Surg Clin Case Rep.* 2023; 6(16): 1-8

Keywords:

ZnO/Fe₂O₃; Nanocomposite; Photocatalytic; Mordant; Congo red; Dye; Textile; Pollutant; Reuse

1. Abstract

The presence of dyes in aqueous media, even in low concentrations caused adverse effects on human, animal, and environmental health. Congo red and mordant dyes are widely used in textile industry and their concentrations were high in the environment. Since non treated dyes cause problems, it appears necessary to remove the dyes from the environment. The current study investigated the congo red and mordant dyes via photocatalysis process using ZnO/Fe₂O₃ nanocomposite as a low-cost catalyst. The effects of variables such as ZnO/Fe₂O₃ nanocomposite dosage, solution pH, initial dye concentration and UV power on dye removal were investigated. For maximum removals of mordant and congo red dyes (99%) the optimal conditions were 500 mg/L individual dye concentrations, 2 mg/L ZnO/Fe₂O₃ nanocomposite dosage, 50 °C temperature, 70 W/m² UV light power, 30 min photodegradation time, pH= 7,00 and after utilization of nanocomposite 19 and 20 runs the dye removals were determined as 97% and 96%. FTIR analyses exhibited that OH groups create an electron and a hole, causing the electron transfer to the dyes and react with the dyes's free radicals. XRD analyses for ZnO and iron oxide samples showed that impurity group containing peaks was not identified. SEM results showed that the ZnO nanoparticles exhibited flower-shaped and ZnO/Fe₂O₃ nanocomposite exhibited an excellent uniformity in particle size distribution. The high photocatalytic activity can be attributed to enhanced charge separation derived from coupling of ZnO and Fe₂O₃. The nanocatalyst was reused 18 times with yields as high as 99%. According to the obtained results, the photocatalytic process in the presence of ZnO/Fe₂O₃ nanocomposite has high efficiency in removing dyes from wastewater sources.

2. Introduction

Most of the living organisms depend on water resources for at least their basic survival. It is a well-known fact that both industrial and human activities produce undesired effects on several natural resources. In this category are included water and wastewater containing pollutants such as dyes [1-5]. As the hazards associated with the more than 100,000 different commercial molecules started to be known, many possible treatments for their removal have appeared. Some water protocols include the removal of pollutants either selectively or not, while other treatments are addressed to not only remove but also destroy the dye to more simple less-hazardous structures [6-12].

There are also several biological, physical, and chemical treatments oriented to achieve dye's removal, and there is a number of materials which have been made available for this same purpose. Some biological and advanced treatment processes were not remove ultimately the dyes and some recalcitrant metabolites released to the environment. Among all the possibilities, nanocomposite materials appear as convenient and promising options and they have demonstrated outstanding capabilities for dyes removal. They are composed of at least two materials: one acting as the filler or reinforcement at the nanoscale, and the other comprises the matrix. Therefore, it is possible to design a composite material according to its desired application, with particular emphasis on its efficiency and capability of reuse [12-20].

Congo red is an organic compound, the sodium salt of 3,3'-([1,1'-biphenyl]-4,4'-diyl)bis(4-aminonaphthalene-1-sulfonic acid). It is an azo dye. Congo red is water-soluble, yielding a red colloidal solution; its solubility is greater in organic solvents. The use of Congo

red in the textile industry has long been abandoned, primarily because of its carcinogenic properties but it is still used for histological staining [18-25]. Mordant dyes are acid dyes having chelating sites to form stable coordination complex with metal ions from metal salts (mordants). Dyes can form chelates with different mordants to develop various shades with superior wash fastness. A mordant or dye fixative is a substance used to set dyes on fabrics. It does this by forming a coordination complex with the dye, which then attaches to the fabric. It may be used for dyeing fabrics or for intensifying stains in cell or tissue preparations. Although mordants are still used, especially by small batch dyers, it has been largely displaced in industry by direct dyes [19-26]. The term mordant comes from the Latin mordere, "to bite". In the past, it was thought that a mordant helped the dye bite onto the fiber so that it would hold fast during washing. A mordant is often a polyvalent metal ion, and one example is chromium (III). The resulting coordination complex of dye and ion is colloidal and can be either acidic or alkaline. Mordants include tannic acid, oxalic acid, alum, chrome alum, sodium chloride, and certain salts of aluminium, chromium, copper, iron, iodine, potassium, sodium, tungsten, and tin. Natural mordant was obtained by concentrating aqueous extract of banana flower petaloids under reduced pressure and evaporating it to dryness. Bharat Merino sheep wool yarn dyed with turmeric (*Curcuma Longa*) was subjected to mordanting separately with natural mordant and chromium under the identical conditions. Out of the different concentrations of the mordants used, 3.5 % natural mordant and 1.5 % chromium (on the weight of yarn) showed similar colour fastness, reflectance, colour shade and K/S values [18-27]. The nanocatalysts serve as a conduit for homogeneous and heterogeneous catalysts due to their highly active surface and capacity to be separated after the reaction [18-29] nanotechnology decreases the quantity of catalyst, energy, and time needed to complete a process. Iron oxide (Fe₂O₃), on the other hand, is appropriate for absorbing wavelengths in the visible light spectrum and has a relatively small energy gap [27-29]. The most significant magnetic benefit of Fe₂O₃ is the ease with which magnetic iron oxide may be readily extracted from solutions using an external magnetic field. Understanding the fundamental features of Fe₂O₃ is


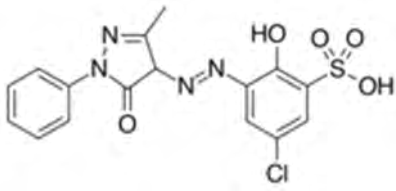
crucial to determine the photoelectric and photochemical properties because different semiconductors have sufficient energy gaps to catalyze a variety of chemical processes [26-29]. Due to their chemical, magnetic, and photoluminescent capabilities, as well as their application as active components in gas sensors. ZnO and Fe₂O₃ have been proposed as luminescence cells in composite particles made of magnetic nuclei. Potential biological and biomedical uses for these composite particles include the detection of cancer cells, germs, and viruses, as well as magnetic isolation. In most of the research related to the photocatalytic degradation of direct blue 199 and basic yellow 28 dyes, ultraviolet light has been used as a source of radiation [18-26]. Ultraviolet light is extremely dangerous for human skin and has a higher economic cost than visible light. Therefore, one of the innovations of this research is the synthesis of photocatalysts with the ability to act against visible light radiation. The supply of raw materials in the photocatalyst synthesis process is from the waste of the filtration unit of the gas pressure reduction station, among other innovations used in this research. With this strategy, the waste cycle of a unit has become a photocatalytic product that can remove environmental pollution [27-29].

In the present study, ZnO/Fe₂O₃ heterojunction has been successfully synthesized under laboratory conditions for photocatalytic degradation of congo red and mordant dyes. The synthesized samples were subjected to XRD, FTIR, SEM, TEM and FESEM for microstructural and morphological investigation. In order to detect the optimal operational conditions for maximum removals of congo red and mordant dyes the effect of increasing ZnO-Fe₂O₃ concentrations (0.5, 1.0, 1.5, 2.0, 2.5 and 3.0 mg/L), dye concentration (50, 100, 150, 200, 300, 500 and 700 mg/l), temperature increase (20, 30, 50 and 70 °C), pH (4-11), UV power (10, 30, 40, 70, 90, 120 and 150 W/m²), photodegradation time (10, 20, 30, 40, 50, 60 and 70 min) were investigated. Furthermore the reusability of the nanocomposite was evaluated.

3. Material and Methods

The formula of congo red and mordant dyes used in this study was tabulated in Table 1.

Table 1: Formula and properties of dyes used in this study

Dyes Formula	
Congo red	Mordant
	
Molecular Formula: C ₃₂ H ₂₂ N ₆ Na ₂ O ₆ S ₂	C ₂₂ H ₁₁ Na ₃ O ₉
Molar weight : 696.665	488.29

3.1. Preparation of the ZnO/Fe₂O₃ nanocomposite

In the preparation of ZnO/Fe₂O₃ nanocomposite, 19.9 mg FeCl₃ and 205 mg ZnO particles were added to 50 mL of deionized water, and the mixture was dispersed at 100 °C for 12.0 h. After cooling to 20 °C, the nanoparticles were separated using centrifugation and washed several times with ethanol and deionized water. The ZnO/Fe₂O₃ nanocomposite was dried at 100°C for 3.0 h and then was used as the catalyst in the photodegradation of dyes [15].

3.2. Measurement of Dyes

The dyes, was quantified by HPLC using a with an Ultimate Plus C18 column (150 mm × 4.6 mm, 5 μm). The mobile phases were a 30:70 (v/v) mixture of methanol and 0.1 mol L⁻¹ acetic acid solution. The HPLC conditions used were as follows: 35°C column temperature, 280 nm detection wavelength, 1.0 mL min⁻¹ flow rate and 5 μL injection volume. Quantification of dye content in each sample was carried out using an established calibration curve of dyes with good linearity (R² = 0.99). All samples and standards were first prepared using 50% methanol as a solvent. For complete release of the dyes, HE-loaded microcapsules were first dispersed in water with 10 minutes of sonication and were then diluted with methanol before analysis.

3.3. Characterization of Congo red and Mordant Dyes

For surface evaluation, FTIR spectroscopy (Germany) was utilized in the frequency range of 200 to 5000 cm⁻¹. The KBr pellet method was used to prepare the sample. The sample to KBr ratio in the synthesized materials was 1:100. In each example, 1 mg of dried material and 100 mg of KBr were homogenized in a transparent tablet at 200 kg/cm for 5 minutes using a mortar and pestle. Powder XRD in the 2-θ extent of 10-80 was performed on the synthesized materials using an advanced XRD diffract meter (Cu K_α, λ = 1.5406). The surface morphology of the samples was studied using a field-emission scanning electron microscope (FESEM: Hitachi). Transmission electron microscopy has been used to examine basic and chemical resources at the nanoscale. TEM analysis were performed in an electron microscope (Olympia) to determine the nanocrystal structure of nanocomposite.

3.4. Samples

The dye samples was taken from a textile industry wastewaters

4. Results and Discussion

4.1. FTIR analysis results of ZnO/ Fe₂O₃ nanocomposite

The peak 3840 cm⁻¹ showed the connection of O-H bonds (Figure 1). The presence of O-H peaks is an indicator to show the increasing of photocatalytic activities. Under certain situations, OH groups create an electron and a hole, causing the electron transfer it to the dyes and react with the dyes's free radicals. The presence of CO₂ in the air causes the 2000 cm⁻¹ peak. Peaks 1200 cm⁻¹

and 605 cm⁻¹ show the production of a ZnO-Fe₂O₃ nanocomposite. Peaks 550 cm⁻¹ and 495 cm⁻¹ reflect the vibrational bonds Fe-O and Zn-O, respectively. SEM analyses were performed for the morphological analysis of nanocomposite.

4.2. XRD analysis of ZnO/ Fe₂O₃ nanocomposite

The XRD pattern for ZnO and iron oxide samples matches to their standard card and no extra impurity-related peak was identified. Diffraction peaks associated with planes (103), (004), (106), (109), (112), (108), (204), (114), (203), (007), (207) for ZnO and diffraction peaks associated with plates (014), (106), (113), (008), (115), (204), (027), (118), (019), (216), (30f) for iron oxides are exhibited in Figure 2. ZnO has a hexagonal crystal structure and has a lattice constant a = b = 3/3142, c = 3/2368, α = β = 35, and γ = 325 and Fe₂O₃ also has a hexagonal crystal structure and has a lattice constant α = β = 35, C = 37/995, a = b = 3/359 and γ = 325. The crystal size of the particles in the ZnO-Fe₂O₃ nanocomposite was determined using the Debay-Scherer relationship and was found to be around 59 nm (data not shown).

4.3. SEM Analysis

Figure 3 (a) and (b) exhibited the SEM images related to ZnO nanoparticles while (d) and (e) showed the pictures of ZnO/Fe₂O₃ nanocomposite. The morphology of ZnO nanoparticles is flower-shaped, like clumps consists of many nanometer sized particles. These nanoparticles have good uniformity in particle size distribution. With the addition of iron oxide nanoparticles and the formation of the nanocomposite, the primary structure of nanoparticles is changed and the particles have a variety of sizes, and due to the nature of magnetic nanoparticles, they assume a lumpy state.

4.4. TEM analysis of ZnO/Fe₂O₃

Figure 4 illustrated an excellent coating of ZnO nanoparticles on the contour of iron oxide nanoparticles. A cluster shape was detected in the ZnO/Fe₂O₃ nanocomposite.

4.5. Effect of Photocatalyst Dosage Photodegradation of Dyes

The effects of photocatalyst dose was taken into consideration by adding 0.5, 1, 1.5, 2, 2.5 and 3 mg/l of ZnO/Fe₂O₃ nanocomposite, and the result demonstrated that increasing the concentration to 2 mg/l increased photodegradation of mordant and congo dyes up to 99% (Table 2). The reason for this is that as the amount of nanocomposite elevated, the number of active sites in the catalyst increasing the degrading efficiency by producing more OH radicals. However, increasing the amount of the catalyst to 3 mg/l cause a turbidity of the studied samples. This decrease the visible light penetration and preventing light from reaching and exciting the catalyst surface. As well as water excitation and no hydroxyl radical formation deteriorates the nanocomposites. This results with lower efficiency.

Table 2: Effect of increasing ZnO/Fe₂O₃ nanocomposite concentration on the photodegradation rates of Mordant and congo dyes

ZnO/Fe ₂ O ₃ nanocomposite concentration (mg/L)	Photodegradation efficiency (%)	
	Mordant dye	Congo red dye
0,5	87	90
1	90	94
1,5	92	96
2	99	99
2,5	90	90
3	76	74

4.6. Effect of Mordant and Congo Dyes Concentrations on Photodegradation of Dyes

The influence of the initial concentration of dyes on photocatalytic degradation performance was examined using 2 mg/L nanocatalysts with varying dye concentrations of 50, 100, 150, 200, 300, 500 and 700 mg/L (Table 3). Increasing the dye concentration from 50 to 700 mg/L reduces the photodegradation efficiency, which might be attributed to the saturation of the active sites in the nanocomposite and lower light penetration. To optimal dye dose for maximum photodegradation was found to be 500 mg/l in both dyes. This dye’s photocatalytic breakdown is nearly complete at its initial concentration. The high concentration of dyes would consume more • OH, so the removal efficiency is reduced with the increase of the initial concentration of mediated contaminants and metabolites . Due to the dyes emoval efficiencies at a concentration of 500 mg/L being a good performance (99%), mordant and congo dye concentration of 500 mg /l was selected as the optimum concentration. By increasing the dye concentration, the driving force also not increase and did not enhances the dye diffusion rate.

4.7. Effect of Temperature on Photodegradation of Mordant and Congo Dyes

Temperature affect the photocatalytic degradation dyes . The temperature was adjusted to 20, 30, 50, and 70 ° C. The data showed that the degradation efficiency both dyes reduced with rising temperature. At high temperature such as 70 ° C deterioration was detected in the stucrure of nanocomposite. To optimal temperature for maximum dye removals was detected at 30 Oc as 99%, however the dye yields was not reduced so much at 50 Oc temperature (97%-98%) (Table 4).

4.8. Effect of UV lighth power

In order to determine to optimal UV lighth power on both dye photodegradation yields the power was increased from 20 W/m² up to 70 W/m², the dyes photodegradation yields was increased from 67% up to 99% as a maximum yield (Table 5). Further increase of lighth power to 90 W/m² and to 180 W/m² the dye yields remained as in 70 W/m². During photodegradation at optimal UV power, catalysts can promote the photodegradation process and generate active free radicals. Consequently, enhancing the photodegradation and mineralization of organic contaminants.

Table 3: Effect of increasing Mordant and congo dye concentrations on their removals

mordant and congo dyes concentrations (mg/L)	Photodegradation efficiency (%)	
	Mordant dye	Congo red dye
50	99	99
100	99	99
150	99	99
200	99	99
300	99	99
500	99	99
700	78	76

Table 4: Effect of increasing temperature on dye removals

Temperature increase (Oc)	Photodegradation efficiency (%)	
	Mordant dye	Congo red dye
20	98	98
30	99	99
50	98	97
70	72	73

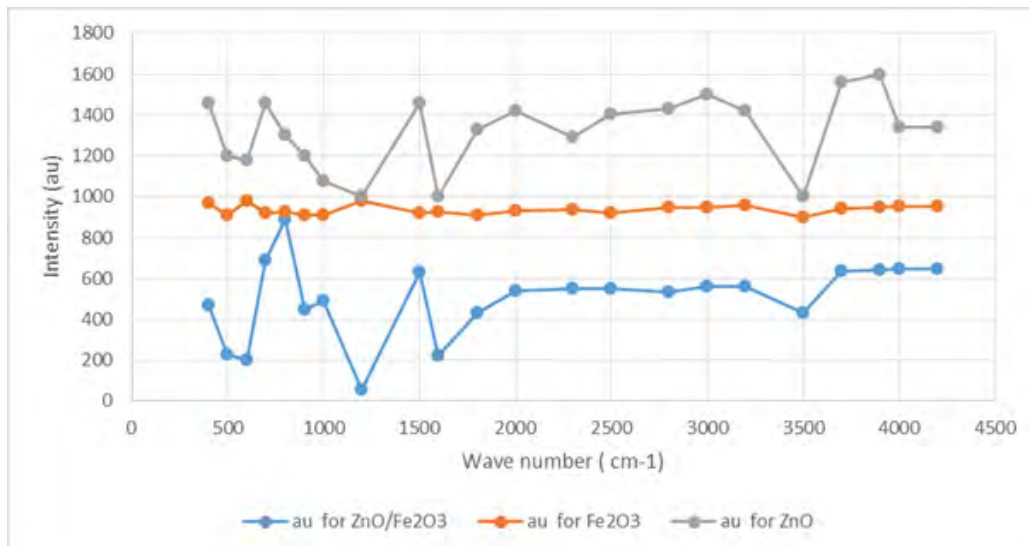


Figure 1: FTIR results for ZnO/ Fe2O3 nanocomposite, ZnO and Fe2O3

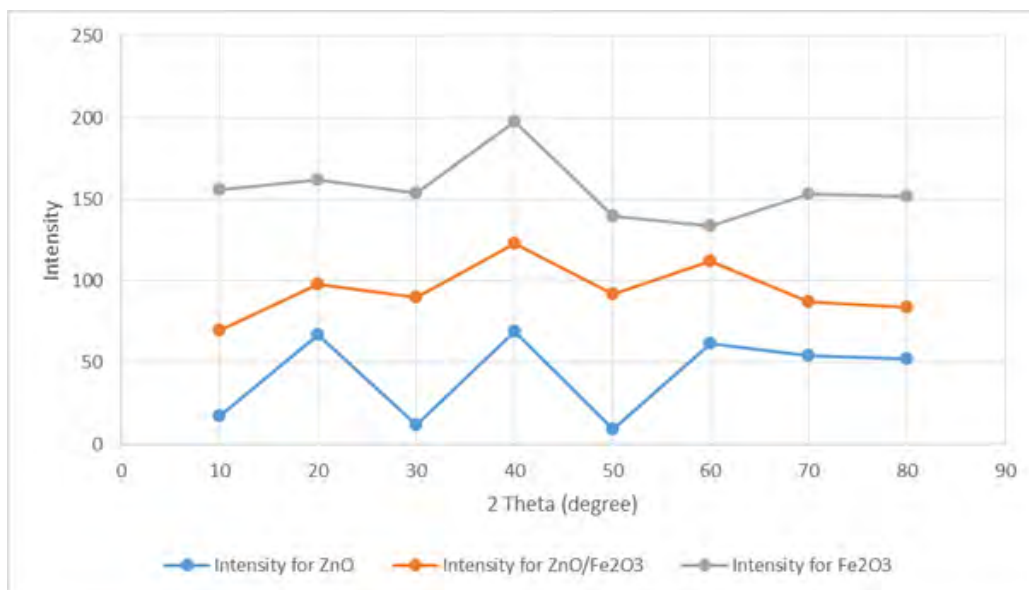
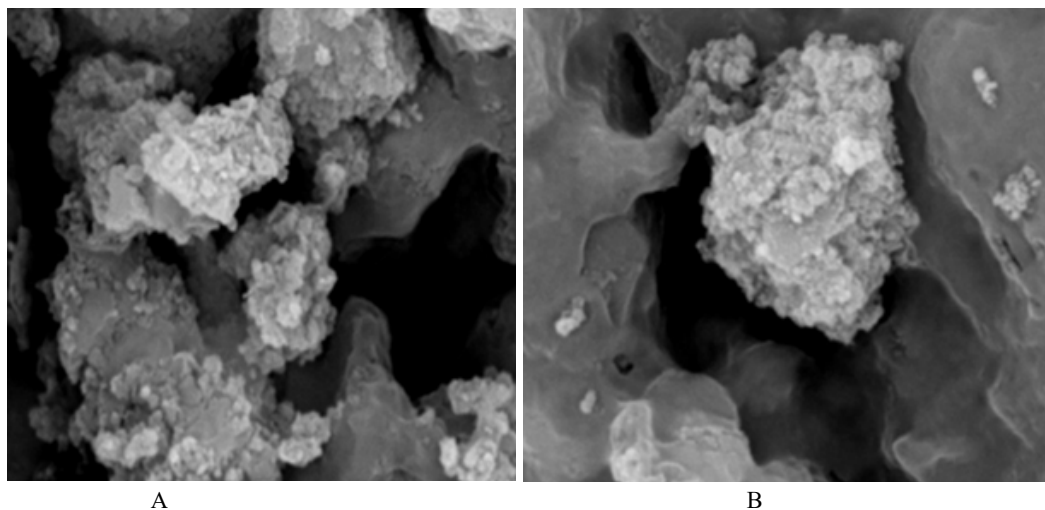


Figure 2: XRD analysis of ZnO/ Fe2O3 nanocomposite, ZnO and Fe2O3



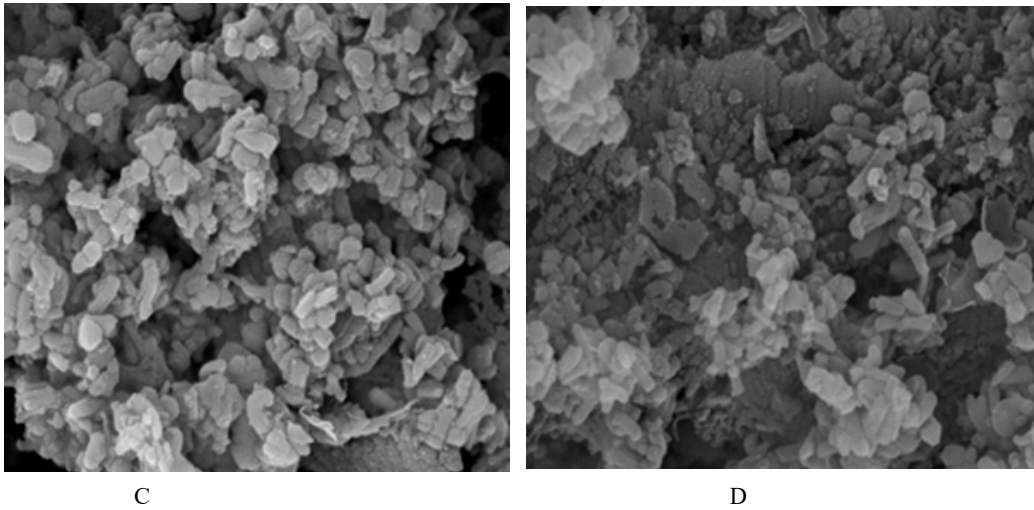


Figure 3: SEM analysis of (a) and (b) of ZnO nanoparticles and (d) and (e) ZnO/Fe₂O₃ nanocomposite.

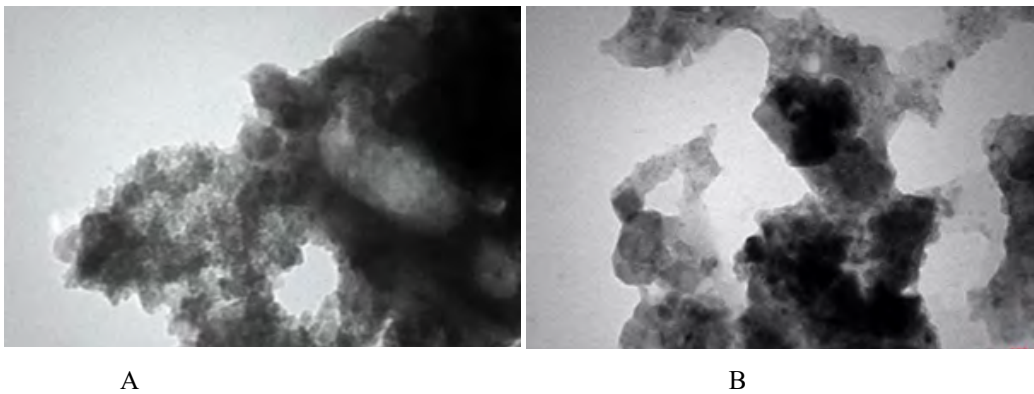


Figure 4: TEM figures of (a, b) ZnO/Fe₂O₃ nanocomposite

Table 5: Effect of increasing UV light power on dye removals

UV light power (W/m ²)	Photodegradation efficiency (%)	
	Mordant dye	Congo red dye
20	67	65
30	78	79
40	90	89
70	99	99
90	99	99
120	99	99
130	99	99

4.9. Effect of photodegradation time on the removal efficiencies of Mordant and congo dyes with 2 mg/l ZnO/ Fe₂O₃ nanocomposite

After 30 min oxidation time the maximum mordant and congo dyes removals were detected as 99% since the adsorption and desorption processes are completed reasonably quickly in the first 30 min (Table 6). Further increase of time did not affect the removals of both dyes. Rapid initial photodegradation is due to the contacts of dye molecules with available activated bonds in the sites of the surface of nanocomposite. Following gradual increasing photodegradation at 30 min may be attributed to the uptake of dyes into

pores of nanocomposite. When binding sites become exhausted, the uptake rate of dyes slows down, and the chance for the availability of active sites decreases.

4.10. Effect of pH on photodegradation of dye removals

The pH of the solution is an essential variable in photocatalytic reactions because it controls the surface charge of the semiconductor photocatalyst. The degradation of both dyes decreased with an increase in pH, which may be the reason for the misplaced adsorption of the product at high pH on the catalyst surface through electrostatic adsorption. The optimal pH for maximum dye removals was found to be 7.0 (Table 7).

Table 6: Effect of increasing time on photodegradation of dye removals

Photodegradation time (min)	Photodegradation efficiency (%)	
	Mordant dye	Congo red dye
10	67	65
20	78	79
30	99	99
40	90	90
50	89	86
60	80	79
70	76	75

Table 7: Effect of increasing pH on dye removals

Ph		Photodegradation efficiency (%)
	Mordant dye	Congo red dye
4	67	65
5	78	79
6	79	78
7	99	99
8	89	86
9	78	70
10	45	45

4.11. Nanocomposite reuse

In the first run the photobiodegradation of dyes was performed with 2 mg/l ZnO/ Fe₂O₃ nanocomposite after 20 min with 99% dye yields. This process was repeated 20 times with the same nanocomposite, and the recovery percentage of this nanoparticle after 18 runs the same dye yields was detected. At run 19 and 20 the yields decreased to 97% and 96%, respectively (Table 8).

Table 8: Nanocomposite reuse

Run		Photodegradation efficiency (%)
	Mordant dye	Congo red dye
1	99	99
2	99	99
3	99	99
4	99	99
5	99	99
19	97	96
20	97	96

5. Conclusions

In this work, a simple method was used to generate a ZnO/Fe₂O₃ nanocomposite. The nanocomposite's morphological and structural characteristics were investigated using XRD, FESEM, SEM and FTIR methods. The maximum photocatalytic activity of the ZnO/Fe₂O₃ nanocomposite to remove the Congo and mordant dyes with yields of 99% were 30 min photodegradation duration, 500 mg/L individual dye concentration, 50 °C temperature, pH = 7.00 and 2 mg/l nanocatalyst dose. The pH, catalyst dosage, dye concentration, and temperature significantly affect the dye yields. The findings demonstrated that although Congo red has a high molecular weight than mordant dye, it was photodegraded with high yields as mordant dye. The benefits of this nanocomposite in the process of degradation of dye molecules include its good photocatalytic action, high stability, and low dosage. Experiment findings indicated that the ZnO-Fe₂O₃ nanocomposite has a substantial ability to degrade the dyes and its usage in the treatment of effluents containing these dyes is suggested.

During photocatalytic degradation, ZnO/Fe₂O₃ nanocomposite

promote effectively the photodegradation process and generate active OH free radicals. The photocatalytic degradation process is an eco-friendly advanced oxidation process and successfully applied to remove the dyes from textile wastes and from polluted water.

References

- Kim I, Yun J, Badloe T, Park H, Seo T, Yang Y, et al. Structural color switching with a doped indium-gallium-zinc-oxide semiconductor. *Photonics Research*. 2020; 8(9): 1409-15.
- Panchal P, Paul DR, Sharma A, Hooda D, Yadav R, Meena P, et al. Phytoextract mediated ZnO/MgO nanocomposites for photocatalytic and antibacterial activities. *Journal of Photochemistry and Photobiology A: Chemistry*. 2019; 385: 112049.
- Bukola D, A. Zaid, E.I. Olalekan, Falilu A. Consequences of anthropogenic activities on fish and the aquatic environment. *Poultry, Fisheries & Wildlife Sciences*. 2015.
- Adegoke KA, Bello OS. Dye sequestration using agricultural wastes as adsorbents. *Water Resources and Industry*. 2015; 12: 8-24.
- El Harfi S, El Harfi A. Classifications, properties and applications of textile dyes: A review. *Applied Journal of Environmental Engineering Science*. 2017; 3(3): 311-320.
- Katheresan V, Kansedo J, Lau SY. Efficiency of various recent wastewater dye removal methods: A review. *Journal of environmental chemical engineering*. 2018; 6(4): 4676-97.
- Arslan, S, Eyvaz M, Gürbulak E, Yüksel E. A review of state-of-the-art technologies in dye-containing wastewater treatment-the textile industry case. *Textile wastewater treatment*. 2016; 1-29.
- Yaseen D, Scholz M. Textile dye wastewater characteristics and constituents of synthetic effluents: a critical review. *International journal of environmental science and technology*. 2019; 16(2): 1193-226.
- Amoli AE, et al. Visible light mediated photocatalytic anionic and cationic dyes degradation. *J. Water Environ. Nanotechnol*. 2023; 8(1): 52-65. Shekofteh-Gohari M, Habibi-Yangjeh A, Abitorabi M, Rouhi A. Magnetically separable nanocomposites based on ZnO and their applications in photocatalytic processes: a review. *Critical Reviews in Environmental Science and Technology*. 2018; 48(10-12): 806-57.
- Varma RS. Journey on greener pathways: from the use of alternate energy inputs and benign reaction media to sustainable applications of nano-catalysts in synthesis and environmental remediation. *Green Chemistry*. 2014; 16(4): 2027-41.
- Hu H, Xin JH, Hu H, Wang X, Miao D, Liu Y. Synthesis and stabilization of metal nanocatalysts for reduction reactions-a review. *Journal of materials chemistry A*. 2015; 3(21): 11157-82.
- Hassanien AS, Akl AA. Optical characteristics of iron oxide thin films prepared by spray pyrolysis technique at different substrate temperatures. *Applied Physics A*. 2018; 124(11): 1-16.
- Wu W, Jiang C, Roy VA. Recent progress in magnetic iron oxide-semiconductor composite nanomaterials as promising photocatalysts. *Nanoscale*. 2015; 7(1): 38-58.

14. Azeredo B, Carton A, Leuvrey C, Kiefer C, Ihawakrim D, Zafairatos S, et al. Synergistic photo optical and magnetic properties of a hybrid nanocomposite consisting of a zinc oxide nanorod array decorated with iron oxide nanoparticles. *Journal of Materials Chemistry C*. 2018; 6(39): 10502-12.
15. Kerli S, Kavgaci M, Soğuksu AK, Avar B. Photocatalytic Degradation of Methylene Blue, Rhodamine-B, and Malachite Green by Ag@ ZnO/TiO₂. *Brazilian Journal of Physics*. 2022; 52(1): 1-11.
16. El-Naggar ME, Shaarawy S, Hebeish A. Multifunctional properties of cotton fabrics coated with in situ synthesis of zinc oxide nanoparticles capped with date seed extract. *Carbohydrate polymers*. 2018; 181: 307-16.
17. Davari N, Farhadian M, Nazar ARS, Homayoonfal M. Degradation of diphenhydramine by the photocatalysts of ZnO/Fe₂O₃ and TiO₂/Fe₂O₃ based on clinoptilolite: structural and operational comparison. *Journal of environmental chemical engineering*. 2017; 5(6): 5707-20.
18. Qing Y, Lang C, Miao X, Jie H, Sheng LL, Chak AT, et al. Cu₂O/BiVO₄ heterostructures: Synthesis and application in simultaneous photocatalytic oxidation of organic dyes and reduction of Cr(VI) under visible light. *Chem. Eng. J*. 2014; 255: 394–402.
19. Adegoke KA, Bello OS. Dye sequestration using agricultural wastes as adsorbents. *Water Resour. Ind*. 2015; 12: 8-24.
20. Ba-Abbad MM, Kadhum AAH, Mohamad AB, Takriff MS, Sopian K. Visible light photocatalytic activity of Fe³⁺-doped ZnO nanoparticle prepared via sol-gel technique. *Chemosphere*. 2013; 91: 1604-11.
21. Navarro S, Fenoll J, Vela N, Ruiz E, Navarro G. Photocatalytic degradation of eight pesticides in leaching water by use of ZnO under natural sunlight. *J. Hazard. Mater*. 2009; 172: 2–3, 1303–1310.
22. Yang L, Dong SY, Sun JH, Feng JL, Wu QH, Sun SP. Microwave-assisted preparation, characterization and photocatalytic properties of a dumbbell-shaped ZnO photocatalyst. *J. Hazard. Mater*. 2010; 179: 438-43.
23. Tian C, Zhang Q, Wu A, Jiang M, Liang Z, Jiang B, Fu H. Cost-effective large-scale synthesis of ZnO photocatalyst with excellent performance for dye photodegradation. *Chem. Commun*. 2012; 48: 2858-60.
24. Lachheb H, Ajala F, Hamrouni A, Houas A, Parrino F, Palmisano L. Electron transfer in ZnO-Fe₂O₃ aqueous slurry systems and its effects on visible light photocatalytic activity. *Catal. Sci. Technol*. 2017; 7: 4041-7.
25. Liu Y, Yu L, Hu Y, Guo C, Zhang F, Lou XWD. A magnetically separable photocatalyst based on nest-like γ -Fe₂O₃/ZnO double-shelled hollow structures with enhanced photocatalytic activity. *Nanoscale*. 2012; 4: 183-7.
26. Wu W, Zhang S, Xiao X, Zhou J, Ren F, Sun L, Jiang C. Controllable synthesis, magnetic properties, and enhanced photocatalytic activity of spindle-like mesoporous α -Fe₂O₃/ZnO core-shell heterostructures. *ACS Appl. Mater. Interfaces*. 2012; 4: 3602-9.
27. Zhang J, Liu X, Wang L, Yang T, Guo X, Wu S, et al. Synthesis and gas sensing properties of α -Fe₂O₃@ZnO core-shell nanospindles. *Nanotechnology*. 2011; 22: 185501.
28. Pang Y, Li Z, Jiao X, Chen D, Li C. Metal-organic framework derived porous α -Fe₂O₃/C nano-shuttles for enhanced visible-light photocatalysis. *ChemistrySelect*. 2020, 5, 1047–1053.
29. Maya-Treviño M, Villanueva-Rodríguez M, Guzmán-Mar J, Hinojosa-Reyes L, Hernández-Ramírez A. Comparison of the solar photocatalytic activity of ZnO-Fe₂O₃ and ZnO-Fe₀ on 2, 4-D degradation in a CPC reactor. *Photochem. Photobiol. Sci*. 2015; 14: 543-9.